Preprints.org

Article

Not peer-reviewed version

Prediction and Transition of Vegetation Vulnerability in the Mara River Basin under Different SSP Scenarios

Wanyi Zhu , Zhenke Zhang * , Shouming Feng , Hang Ren

Posted Date: 4 March 2024

doi: 10.20944/preprints202403.0044.v1

Keywords: Mara River basin; Vegetation vulnerability; Shared Socio-Economic Pathways (SSPs); Prediction; Stochastic matrix

Preprints.org is a free multidiscipline platform providing preprint service that is dedicated to making early versions of research outputs permanently available and citable. Preprints posted at Preprints.org appear in Web of Science, Crossref, Google Scholar, Scilit, Europe PMC.

Copyright: This is an open access article distributed under the Creative Commons Attribution License which permits unrestricted use, distribution, and reproduction in any medium, provided the original work is properly cited.

Preprints.org (www.preprints.org) | NOT PEER-REVIEWED | Posted: 4 March 2024 doi:10.20944/preprints202403.0044.v1

Disclaimer/Publisher's Note: The statements, opinions, and data contained in all publications are solely those of the individual author(s) and contributor(s) and not of MDPI and/or the editor(s). MDPI and/or the editor(s) disclaim responsibility for any injury to people or property resulting from any ideas, methods, instructions, or products referred to in the content.

Article

Prediction and Transition of Vegetation Vulnerability in the Mara River Basin under Different SSP Scenarios

Wanyi Zhu [1,2], Zhenke Zhang [1,2,*], Shouming Feng [1,2] and Hang Ren [3]

1 School of Geography and Ocean Science, Nanjing University, Nanjing 210023, China; 602023270074@smail.nju.edu.cn (W.Z.); fengsm@smail.nju.edu.cn (S.F.)
2 Institute of African Studies, Nanjing University, Nanjing 210023, China
3 Institute of Population Studies, Nanjing University of Posts and Telecommunications, Nanjing 210042, China; rh@njupt.edu.cn (H.R.)
* Correspondence: zhangzk@nju.edu.cn.

Abstract: The Mara River basin (MRB) has a world-famous ecosystem, but the vegetation has been damaged due to economic development in recent years, and there is little known about the area that will experience severe vegetation damage in the future. Based on the vegetation vulnerability system, principal component analysis, and three CMIP6 scenarios (SSP1-2.6, SSP2-4.5, SSP5-8.5), vegetation vulnerability was calculated in the base period (2010-2019), near-term period (2020-2059) and long-term period (2060-2099) in the MRB. The spatial cluster of vegetation vulnerability was revealed by spatial correlation analysis, and the transition of vegetation vulnerability of different periods was analyzed by stochastic matrix. The results showed that in all periods, the vulnerability showed a high-high cluster in the east, and a low-low cluster midstream and downstream. From the stochastic matrix, the area of high vulnerability increased the least under the SSP1-2.6, while it increased the most under the SSP5-8.5. The vegetation vulnerability upstream increased the most from the base period to the near-term period and long-term period in the MRB. By comparing the vegetation vulnerability under different scenarios, and pointing out the areas with the highest vulnerability increase, this study can better provide comprehensive decision-making for vegetation protection in the MRB.

Keywords: Mara River basin; vegetation vulnerability; shared socio-economic pathways (SSPs); prediction; stochastic matrix

1. Introduction

The fierce global warming and human activities have had significant impacts on vegetation [1], and vegetation degradation is an important external expression of vulnerability [2]. Land use changes and intensified environmental pollution caused by human activities can both result in vegetation degradation [3,4] and further increase vegetation vulnerability. Also, continuous global warming can increase the vulnerability of 50% of vegetation on Earth [5]. In the 21st century, where climate change and human activities are more complex, vegetation vulnerability is more serious [6].

The concept of 'vulnerability' is defined as "the degree to which a system, sub-system, or system component is likely to experience harm due to exposure to a hazard, either a perturbation or a stress/stressor" [7]. The commonly used quantitative vulnerability assessment frameworks are the analytic hierarchy process [8] and principal component analysis [9]. Principal component analysis can achieve data transformation by transforming multiple high-correlation variables into minority low-correlation variables through orthogonal transformation and is more used in assessment frameworks with both natural factors and human factors [9]. With the development and application of GIS and RS technology, vulnerability assessment systems have become more objective, and visual expression makes vulnerability more intuitive [10]. Current researches on vegetation vulnerability are mostly based on the changes in net primary productivity (NPP) and gross primary productivity

© 2024 by the author(s). Distributed under a Creative Commons CC BY license.

Preprints.org (www.preprints.org) | NOT PEER-REVIEWED | Posted: 4 March 2024 doi:10.20944/preprints202403.0044.v1

(GPP) [11]. Few studies comprehensively assess vegetation vulnerability by constructing indicator systems.

There have been many studies focusing on the impact of future climate change on vulnerability. These studies used assumed incremental scenarios (average temperature and precipitation increasing equidistant from baseline to the future) [12] and GCMs (general circulation models) [13] as the main input data. However, the spatiotemporal resolution of data in existing research is relatively rough. Most prediction models do not take the impact of human activities on vulnerability into consideration and only use a single climate change scenario, which increases the uncertainty of prediction. The CMIP6 dataset is currently the most accurate and high spatiotemporal resolution dataset for simulating future climate change, and SSP1-2.6, SSP2-4.5, and SSP5-8.5 are taken to be representatives of low-, medium-, and high-emission scenarios, respectively [14]. It can reflect the comprehensive effects of climate and socio-economic factors and has been widely used in predicting future land use patterns [15]. However, the CMIP6 dataset is barely applied to predict vegetation vulnerability.

In the past few decades, vegetation in sub-Saharan Africa has experienced extensive degradation [16]. The Mara River Basin (MRB) is one of the most serious vegetation degradation areas due to the intensive deforestation, tourism, and mining since the 1970s [17,18,19]. The rapid growth of the population in MRB has led to a soaring demand for agriculture and animal husbandry, which destroys much natural vegetation [20,21]. The vegetation degradation increases the vegetation vulnerability in the MBR. In addition, the terrain fluctuation exceeds 1000m in the MRB, and the huge terrain fluctuation makes vegetation habitats complex and more susceptible to climate change and human activities, posing a threat to vegetation vulnerability [9]. Considering the climate and human activities will be more complex in the 21st century [22], it is necessary to know the future vegetation vulnerability in advance to protect natural vegetation in MRB.

The vulnerability threat caused by vegetation degradation has been studied in many regions, and RS and GIS are important methods for studying vegetation vulnerability in areas with limited data. The researches on vegetation in the MRB mainly focus on the mapping of vegetation types [23], the response of vegetation to climate change [24], and the calculation of vegetation ecological water demand [25], trying to understand the changes of vegetation under natural and socio-economic changes [26,27]. However, there are relatively few researches studying vegetation vulnerability. Therefore, taking 2010-2019 as the base period, evenly divided the remaining years of the 21st century as near-term period (2020-2059) and long-term period (2060-2099), vegetation vulnerability system, principal component analysis, and three CMIP6 scenarios (SSP1-2.6, SSP2-4.5, SSP5-8.5) were used to assess vegetation vulnerability in the MRB. Then the spatial cluster of vegetation vulnerability was revealed by spatial correlation analysis, and the stochastic matrix was used to analyze the transition of vegetation vulnerability among the base period, near-term period, and long-term period. This study aims to provide a comprehensive understanding of vegetation vulnerability and point out the areas with severe vulnerability in the future to provide scientific support and comprehensive decision-making for vegetation protection in the MRB.

2. Study Area

The Mara River originates from the Mau Forest in Kenya, through the Masai Mara National Reserve, Serengeti National Reserve, and finally flows into Lake Victoria, with an area of 13750 km2 (Figure 1). The upstream contains national forest reserve and agricultural reclamations. The midstream includes two national wildlife reserves, Masai Mara National Reserve (Kenya) and Serengeti National Reserve (Tanzania). The downstream is the Mara Wetland and other sparse grassland [28]. The vegetation distribution changes significantly from the upstream to the downstream in the MBR, from alpine forest, and scattered forest to cultivated land, and then to grassland, shrub, mixed shrub, and grassland. The main vegetation types are forest, crop, grassland, and shrub. The MRB is the home of many wild animals and has important ecological value.

Preprints.org (www.preprints.org) | NOT PEER-REVIEWED | Posted: 4 March 2024 doi:10.20944/preprints202403.0044.v1

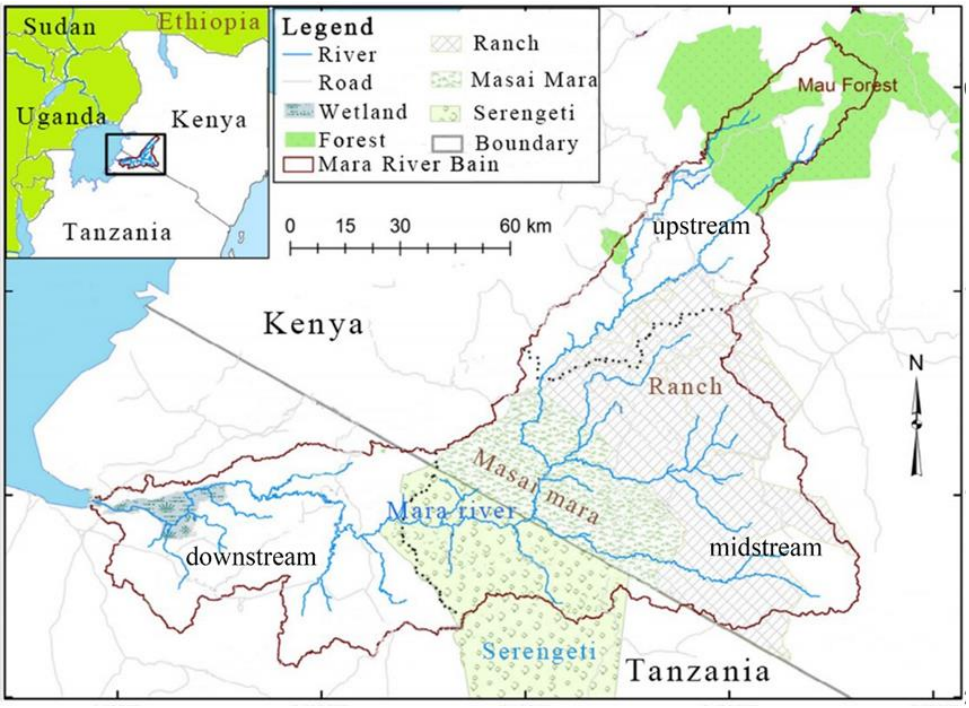

Figure 1. The location of MRB.

3. Methods and Data

3.1. Methods

The vegetation vulnerability analysis was constructed by principal component analysis based on natural and human factors. Then Moran's I was used to measure the spatial cluster of vegetation vulnerability in the base period, near-term period, and long-term period. Finally, the stochastic matrix was used to quantitatively analyze the transition of vegetation vulnerability from the base period to the near-term period and the long-term period.

3.1.1. Scenario Assumptions

Among the 5 shared socio-economic paths (SSP1-SSP5) in CMIP6, SSP1-2.6, SSP2-4.5, and SSP5-8.5 are the representatives of low-, medium-, and high-emission scenarios [14]. This study used SSP1-2.6, SSP2-4.5, and SSP5-8.5 to predict vegetation vulnerability and to explore the impact of emission on vegetation vulnerability in the near-term period and the long-term period in the MRB.

3.1.2. Factors

Vegetation vulnerability is impacted by both natural and human factors. Natural factors are the basis for vegetation growth and survival, including climate, terrain, and water [29]. Human factors mainly refer to the external pressure from socio-economic development [30]. Based on the problems faced by vegetation in the MRB, 4 natural factors and 2 human factors were selected to construct the vegetation vulnerability system for the base period, near-term period, and long-term period (Table 1).

Table 1. Vegetation vulnerability factors.

Factors	Index	Unit	Property
Natural factors	Precipitation	mm	-
	Temperature	℃	-
	Terrain	m	+
	Vegetation ecological water	m^3	-

Preprints.org (www.preprints.org) | NOT PEER-REVIEWED | Posted: 4 March 2024 doi:10.20944/preprints202403.0044.v1

Human factors	Population density	person/km²	+
	Land use	%	+

The land use degree reflects the degree of land utilization, it can also reflect the pressure of human activities on land. The land use degree can be calculated by formula (1) [31]:

$$L = 100 \times \sum_{i=1}^{n} A_i P_i / A_T \quad (1)$$

Where L is the land use degree. n is the number of land use types, and it was 4 in this study. A_i is the area of i land use type. A_T is the total area of the study area. P_i is the parameter for land use degree, it can reflect the intensity and characteristics of human activities. Delphi scoring method and Leopold matrix method were combined to determine the parameter of land use degree (P_i) by taking the mean value of the two methods (Table 2) [31].

Table 2. Land use degree parameters (P_i) for different land use types in the MRB.

Farmland	Forest	Grass	Shrub
0.71	0.17	0.29	0.29

3.1.3. Vegetation Vulnerability

1. Data standardization

Due to the units and properties being different, the original data were standardized for easier subsequent calculations. The positive indexes (2) and negative indexes (3) were calculated by different standardized calculation formulas:

$$Z_i = \frac{X_i - X_{min}}{X_{max} - X_{min}} \quad (2)$$

$$Z_i = \frac{X_{max} - X_i}{X_{max} - X_{min}} \quad (3)$$

Where Z_i is the standardized value of the index i. X_i is the original value i. X_{max} is the maximum value of i, and X_{min} is the minimum value.

2. Vegetation vulnerability

Principal component analysis can maximize the retention of information reflected by multiple variables, it was used to calculate vegetation vulnerability. The vegetation vulnerability was calculated by:

$$EVI = a_1 F_1 + a_2 F_2 + \cdots + a_n F_n \quad (4)$$

Where EVI is the vegetation vulnerability, a_i is the importance of index I and F_i is the index i.

3. Spatial cluster of vegetation vulnerability

To analyze the spatial cluster of vegetation vulnerability in the MRB, global Moran's I was used to measure whether there was a spatial cluster of vegetation vulnerability, and local Moran's I was used to measure the spatial cluster pattern of vegetation vulnerability.

Global Moran's I can be calculated as:

$$I_g = \frac{\sum_{i=1}^{n}\sum_{j=1}^{n} w_{ij}(x_i - \bar{x})(x_j - \bar{x})}{\sum_{i=1}^{n}\sum_{j=1}^{n} w_{ij}(x_i - \bar{x})^2} \quad (5)$$

Local Moran's I can be calculated as:

$$I_l = \frac{(x_i - \bar{x})}{S^2} \sum_{j=1}^{n} w_{ij}(x_j - \bar{x}) \quad (6)$$

Where x_i and x_j are the vulnerability values of the i and j regions, $\bar{x}$ is the average vulnerability value of all regions. w_{ij} is the spatial weight matrix. S is the sum of the elements of the spatial weight matrix. n is the number of regions. A Local Indicators of Spatial Association (LISA) of vegetation

Preprints.org (www.preprints.org) | NOT PEER-REVIEWED | Posted: 4 March 2024 doi:10.20944/preprints202403.0044.v1

vulnerability can be obtained by clustering the local Moran's *I*. The LISA has five cluster patterns, namely high-high cluster (H-H), high-low outlier (H-L), low-high outlier (L-H), low-low cluster (L-L), and not significant.

3.1.4. Transition of Vegetation Vulnerability

The stochastic matrix was used to better reflect the transition of vegetation vulnerability of different periods in the MRB. The stochastic matrix can be calculated by:

$$S_{ij} = \begin{bmatrix} S_{11} & \cdots & S_{1n} \\ \vdots & \ddots & \vdots \\ S_{n1} & \cdots & S_{nn} \end{bmatrix} \quad (7)$$

where n is the vegetation vulnerability. S_{ij} (i, j=1,2,3,..., n) is the transition area that transfers from the vulnerability i at the beginning to the vulnerability j at the end (unit: km^2). The i=j indicates that the vulnerability has not changed during the period.

3.2. Data

The data used include climate, terrain, population, land use, and vegetation ecological water. The terrain data was from STRM. The rest data includes two parts, the details are as follows. All data was resampled to resolution of 1km by bilinear interpolation method

1. Climate. The temperature and precipitation data in the base period were obtained from ERA5-Land monthly average reanalysis data. Due to the study area is not large and the data needed for predicting future vegetation ecological water should include radiation, temperature, precipitation, wind speed, and humidity, the CNRM-CM6-1-HR model in the CMIP6 dataset under SSP1-2.6, SSP2-4.5, and SSP5-8.5 was chosen for including all the above elements and having a relatively small spatial resolution.

2. Land use. The land use data for the base period were obtained from the European Space Agency, the land type accounted for the largest proportion in a grid was taken as the land use type for that grid. The land use data for the near-term period and long-term period under SSP1-2.6, SSP2-4.5, and SSP5-8.5 were from Land Use Harmonization 2 (LUH2).

3. Population. The population data in the base period was sourced from the WorldPop population density dataset. According to Our World in Data, the population growth rate in Kenya from 2020 to 3030 is about 2.0%, from 2030 to 2059 is about 1.3%, and from 2060 to 2099 is about 0.3%. The population growth rate in Tanzania from 2020 to 3030 is about 2.8%, from 2030 to 2059 is about 2.1%, and from 2060 to 2099 is about 1.0%. The average population growth rate of Kenya and Tanzania was taken as the population growth rate of MRB. Therefore, the population growth rate of the MRB from 2020 to 3030 is about 2.4%, from 2030 to 2059 is about 1.7%, from 2060 to 2099 is about 0.7%, and the population density was shown in Table 3.

Table 3. Population density of near-term period and long-term period in MRB.

	2019	**2020-2059**	**2060-2099**
Population density/person •km^{-2}	121.17	197.79	261.45

4. Vegetation ecological water. The vegetation ecological water of the base period was from the research results [25]. The vegetation ecological water under SSP1-2.6, SSP2-4.5, and SSP5-8.5 of the near-term period and long-term period were calculated by the RF algorithm with terrain and CMIP6 data. The minimum R^2 in all scenarios is 0.74, indicating good results (Figure 2).

Preprints.org (www.preprints.org) | NOT PEER-REVIEWED | Posted: 4 March 2024 doi:10.20944/preprints202403.0044.v1

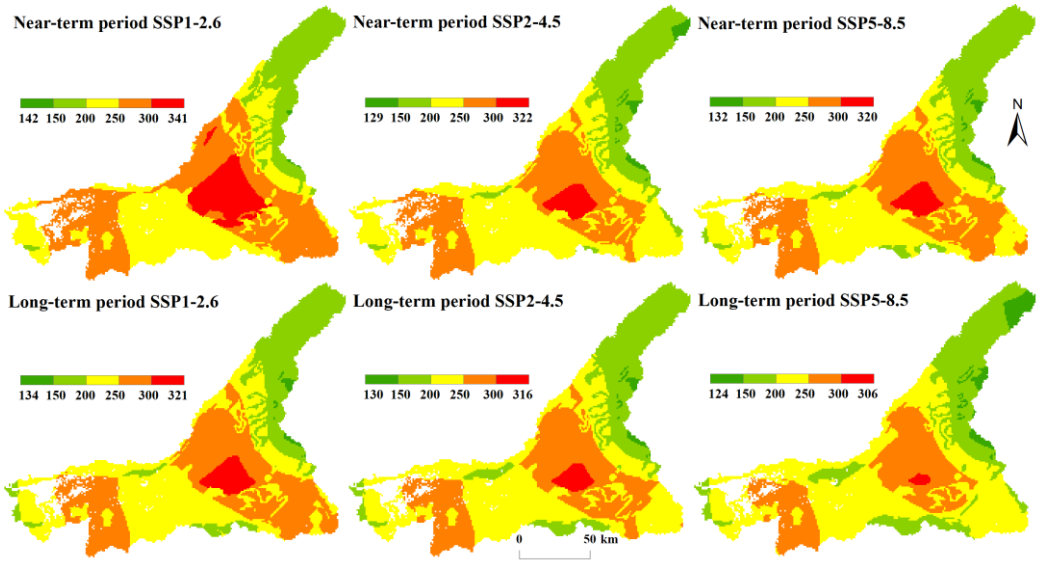

Figure 2. Vegetation ecological water (unit:$10^{10}m^3$) of near-term period and long-term period in MRB.

4. Results

4.1. Factor Scores

The scores of natural and human factors were shown in Table 4, the factor scores varied greatly in different periods. Natural factors scored higher than human factors in all periods, and temperature got the biggest negative score, land use got the biggest positive score. From the low to high emission scenarios, the score of population increased rapidly, and the score of vegetation decreased.

Table 4. Natural and human factor scores of different periods in MRB.

Factors	Base period	Near-term period			Long-term period		
		SSP1-2.6	SSP2-4.5	SSP5-8.5	SSP1-2.6	SSP2-4.5	SSP5-8.5
Precipitation	-0.67	-0.69	-0.62	-0.56	-0.69	-0.65	-0.60
Temperature	-0.79	-0.85	-0.80	-0.75	-0.86	-0.84	-0.79
Terrain	0.77	0.81	0.80	0.83	0.82	0.81	0.87
Vegetation	-0.61	-0.63	-0.60	-0.50	-0.66	-0.62	-0.51
Population	0.60	0.59	0.70	0.83	0.68	0.78	0.89
Landuse	0.78	0.64	0.70	0.72	0.74	0.80	0.87

In the base period, temperature got the biggest negative score, and land use and terrain got the biggest positive score. Precipitation and temperature were factors that contributed significantly to vegetation vulnerability in the near-term period and long-term period. From low to high emission scenarios, in the near-term period, the scores of precipitation, temperature, and vegetation decreased, while the scores of land use and population increased. The situation was the same in the long-term period.

4.2. Vegetation Vulnerability and Spatial Cluster in the Base Period in MRB

Figure 3a showed the spatial distribution of vegetation vulnerability in the base period in MRB. The natural breakpoint method was used to divide the vegetation vulnerability into four categories, namely mild vulnerability, moderate vulnerability, severe vulnerability, and extreme vulnerability. In the base period, extreme vulnerability was in the east part of MRB, and mild vulnerability was in the downstream. There was a decreasing trend in vegetation vulnerability from east to west in the MRB.

Preprints.org (www.preprints.org) | NOT PEER-REVIEWED | Posted: 4 March 2024 doi:10.20944/preprints202403.0044.v1

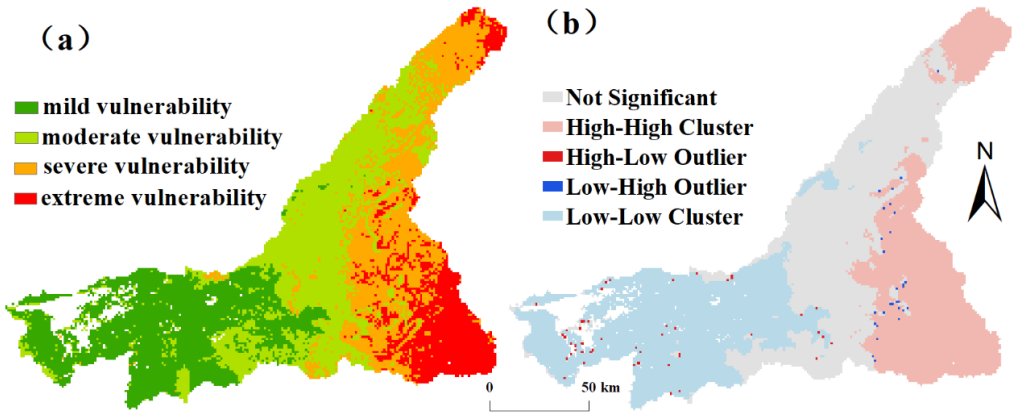

Figure 3. Spatial distribution of vegetation vulnerability (a), and LISA cluster (b) in the base period in the MRB.

The global Moran's *I* of vegetation vulnerability in the base period was 0.7868, the *Z*-value was 26.1325, the variance was 0.0009, and the *P*-value was less than 0.01, indicating significant results at the 99% level. This indicated a strong positive correlation between vegetation vulnerability and geographical location (Figure 3b). Specifically, severe vulnerability and extreme vulnerability were mostly in the high-high cluster, while mild vulnerability was almost in the low-low cluster.

4.3. Vegetation Vulnerability in the Near-Term and Long-Term Period in MRB

The vegetation vulnerability in the near-term period and long-term period showed a decreasing trend from the upstream to the downstream, with the center being the smallest (Figure 4). In the near-term period, from low to high emission scenarios, the area of mild vulnerability and moderate vulnerability decreased about 6%, the area of extreme vulnerability increased by about 8%. In the long-term period, from low to high emission scenarios, the area of mild vulnerability decreased by about 50%, and the area of severe vulnerability increased by about 20%.

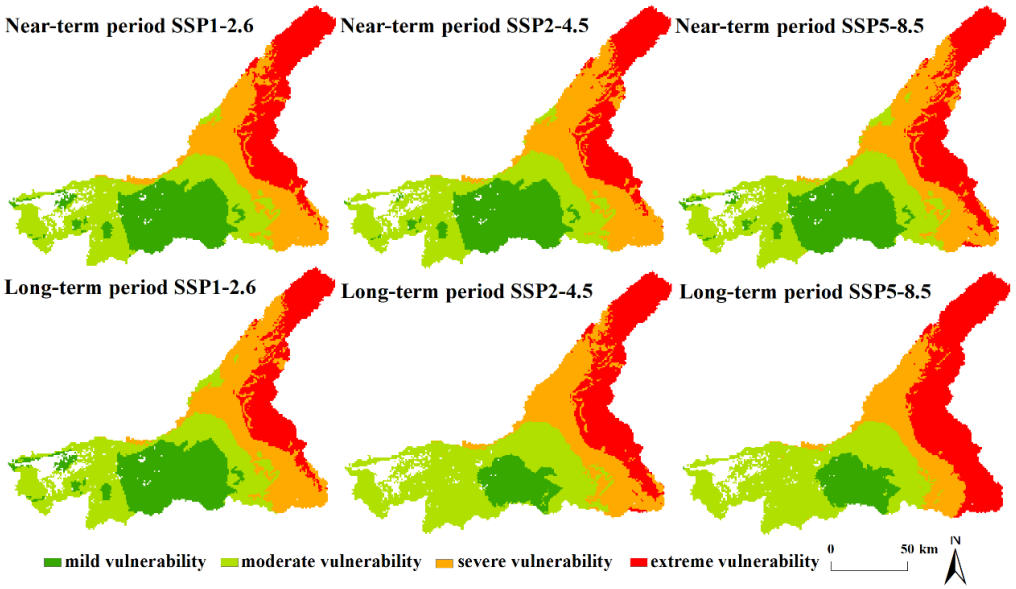

Figure 4. Spatial distribution of vegetation vulnerability in the near-term period and the long-term period in the MRB.

From the near-term period to the long-term period, under the SSP1-2.6, the area of severe vulnerability increased by about 6%, and the area of extreme and mild vulnerability decreased by about 16% and 12% respectively. Under the SSP2-4.5, the area of mild vulnerability decreased by about 56%, and the area of extreme vulnerability increased by about 33%. Under the SSP5-8.5, the

Preprints.org (www.preprints.org) | NOT PEER-REVIEWED | Posted: 4 March 2024 doi:10.20944/preprints202403.0044.v1

area of mild vulnerability decreased by 50%, and the area of severe vulnerability and extreme vulnerability increased by 20% and 40%, respectively. The vegetation vulnerability increased faster under higher emission scenarios from the near-term period to the long-term period.

4.4. Spatial Cluster of Vegetation Vulnerability in the Near-Term Period and the Long-Term Period in the MRB

4.4.1. Global Moran's I

Table 5 showed the results of global Moran's *I* of vegetation vulnerability in the MRB in the near-term period and long-term period. The Moran's *I* was positive in all scenarios, fluctuating between 0.41 and 0.68. The *P*-values were less than 0.01, indicating significant results at the 99% level. This indicated a strong positive correlation between vegetation vulnerability and geographical location in the MRB in the near-term period and long-term period.

Table 5. Global Moran's *I*.

Period	Scenario	Global Moran's *I*	*P*-value	*Z*-value	Variance
Near term period	SSP1-2.6	0.5963	*P*<0.01	12.9971	0.0021
	SSP2-4.5	0.6077	*P*<0.01	13.4134	0.0021
	SSP5-8.5	0.6028	*P*<0.01	11.2632	0.0029
Long-term period	SSP1-2.6	0.5024	*P*<0.01	11.0596	0.0021
	SSP2-4.5	0.4108	*P*<0.01	8.8842	0.0021
	SSP5-8.5	0.4811	*P*<0.01	10.7101	0.0020

4.4.2. Local Moran's I

The LISA cluster of vegetation vulnerability in the near-term period and long-term period in the MRB was shown in Figure 5. The cluster pattern of vegetation vulnerability was a high-high cluster upstream, low-low cluster downstream, not significant midstream in the near-term period and long-term period in the MRB. There were no high-low outlier and low-high outlier, which indicated that the cluster of vegetation vulnerability was extremely concentrated in the near-term period and long-term period in the MRB. Specifically, the high vegetation vulnerability was in the high-high cluster upstream, the low vulnerability was in the low-low cluster downstream.

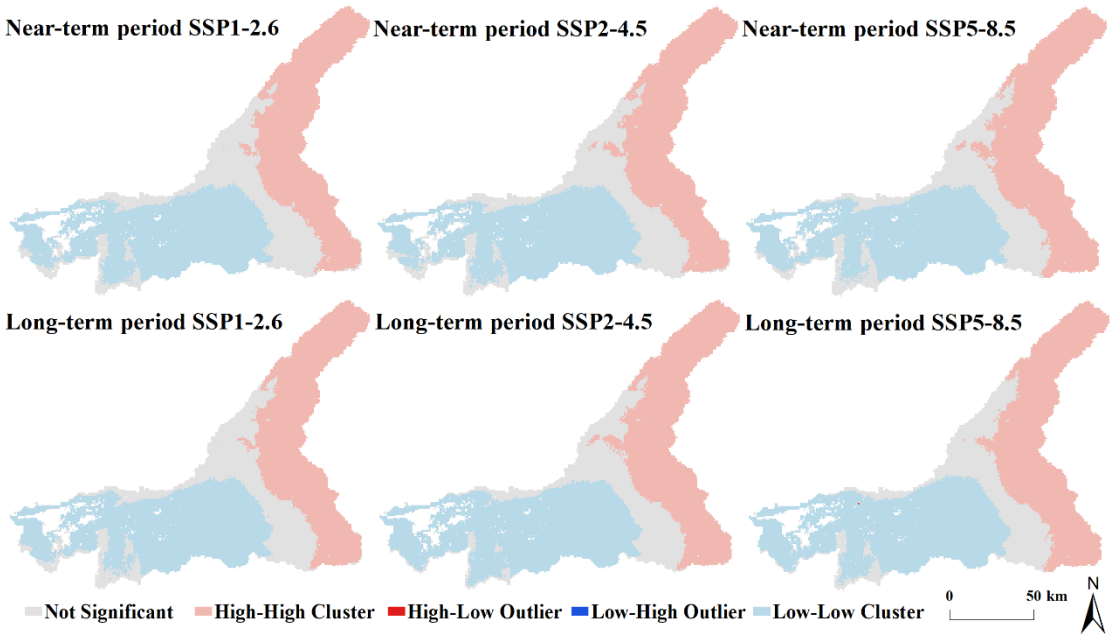

Preprints.org (www.preprints.org) | NOT PEER-REVIEWED | Posted: 4 March 2024 doi:10.20944/preprints202403.0044.v1

Figure 5. LISA cluster of vegetation vulnerability in the near-term period and long-term period in the MRB.

From low to high emission scenarios, the area of high-high cluster increased, and the area of low-low cluster decreased. This changing trend was more obvious in the long-term period. Under the SSP1-2.6, from the near-term period to the long-term period, the area of the high-high cluster decreased upstream, and the low-low cluster increased downstream. The situation was similar under the SSP2-4.5, but the changing areas were larger than the SSP1-2.6. Under the SSP5-8.5, from the near-term period to the long-term period, the area of high-high cluster and low-low cluster were both increased. This indicated that from the near-term period to the long-term period, the vegetation vulnerability could be reduced under a low-emission scenario.

4.5. Transition of Vegetation Vulnerability during Different Periods in the MRB

Table 6 showed the transition of vegetation vulnerability during different periods. From the base period to the near-term period, under the SSP1-2.6, the mild vulnerability, moderate vulnerability, and severe vulnerability had the largest transition area into moderate vulnerability, severe vulnerability, and extreme vulnerability respectively, with the area all over 1200 km^2. The transition area from extreme vulnerability to severe vulnerability was twice the area where extreme vulnerability remained unchanged. Under the SSP2-4.5, the mild vulnerability, moderate vulnerability, and severe vulnerability still had the largest transition area into moderate vulnerability, severe vulnerability, and extreme vulnerability respectively, but the transition area increased 100 km^2 compared to the SSP1-2.6. The transition area of extreme vulnerability to severe vulnerability decreased by 50 km^2 compared to the SSP1-2.6. Under the SSP5-8.5, the transition area of mild vulnerability, moderate vulnerability to severe vulnerability, and extreme vulnerability increased more rapidly compared to the SSP1-2.6 and SSP2-4.5. The area of extreme vulnerability remained unchanged was the largest compared to the SSP1-2.6 and SSP2-4.5.

Table 6. Stochastic matrix of vegetation vulnerability of different periods in MRB.

		Base period			
		mild	moderate	severe	extreme
Near-term SSP1-2.6	mild	1427.61	1057.06	73.70	0.08
	moderate	1676.52	1379.37	503.02	86.39
	severe	22.74	1289.47	464.29	954.46
	extreme	0.00	106.47	1559.48	455.86
Near-term SSP2-4.5	mild	1351.47	1024.37	73.73	0.13
	moderate	1752.05	1041.04	415.79	102.43
	severe	24.24	1496.44	424.03	901.02
	extreme	0.00	170.01	1687.06	493.15
Near-term SSP5-8.5	mild	1338.22	979.58	68.75	0.05
	moderate	1752.92	959.38	309.23	73.93
	severe	36.71	1413.57	544.01	795.42
	extreme	0.00	379.88	1678.56	625.36
Long-term SSP1-2.6	mild	1459.88	1094.89	76.52	0.13
	moderate	1660.31	1041.00	513.20	86.40
	severe	7.25	1410.49	585.67	836.62
	extreme	0.00	187.05	1425.16	573.64
Long-term	mild	577.33	480.51	28.75	0.00

Preprints.org (www.preprints.org) | NOT PEER-REVIEWED | Posted: 4 March 2024 doi:10.20944/preprints202403.0044.v1

SSP2-4.5	moderate	2535.59	1406.58	445.61	35.13
	severe	16.63	1435.84	496.37	780.14
	extreme	0.00	407.28	1628.81	679.34
Long-term SSP5-8.5	mild	506.43	502.26	40.70	0.00
	moderate	2604.85	983.15	293.66	15.30
	severe	18.47	1584.28	493.95	373.88
	extreme	0.00	660.82	1771.22	1108.06

From the base period to the long-term period, under the SSP1-2.6, the area of mild vulnerability transformed into moderate vulnerability unchanged was almost the same as the area of unchanged mild vulnerability. Similarly, the area of moderate vulnerability transformed into mild vulnerability was almost the same as the area of unchanged moderate vulnerability, but smaller than the area that moderate vulnerability transformed into severe vulnerability. Compared with the base period to the near-term period, the transition area of severe vulnerability to extreme vulnerability was much less, and the transition area of extreme vulnerability to severe vulnerability was a little less. Under the SSP2-4.5, compared with the base period to the near-term period, the transition area of mild vulnerability to moderate vulnerability increased by about 800 km^2. The area transformed from moderate vulnerability to mild vulnerability decreased obviously, but the area from moderate vulnerability transformed to extreme vulnerability increased by 139.41%. The area of unchanged extreme vulnerability increased by 37.73%. Under the SSP5-8.5, the vegetation vulnerability transition was similar to the SSP2-4.5. Compared with the base period to the near-term period, the area of mild vulnerability, moderate vulnerability, and severe vulnerability transformed to moderate vulnerability, severe vulnerability, and extreme vulnerability all increased by about 100 km^2. In addition, the area of unchanged extreme vulnerability increased by 77.28% compared with the base period to the near-term period.

Under all scenarios, from the base period to the near-term period or to the long-term period, there was no transition between mild vulnerability and extreme vulnerability. From low to high emission scenarios, the area of unchanged vulnerability or less vulnerability gradually decreased, and the area transformed into higher vulnerability increased. From the near-term period to the long-term period, the transition to higher vulnerability became much more obvious, and the transition increased fast under a high emission scenario.

5. Discussion

5.1. Effects of Factors on Vegetation Vulnerability in the MRB

Mara River Basin is a vegetation vulnerability area in East Africa, and the balance between social development and vegetation protection is not good [23]. The Mau Forest in the upstream was severe vulnerability in the base period and was extreme vulnerability in the near-term period and long-term period. In recent years, the Mau Forest has been extensively cultivated into farmland for agricultural development [17], increasing the vegetation vulnerability of the forest. Therefore, under the SSP5-8.5, which is the most significant scenario for human activities, so the vegetation vulnerability increased the most upstream of the MRB. There are many protected areas midstream and human activities are relatively less [32], but as the emission increased, the area of mild vulnerability decreased obviously in the near-term period and long-term period, indicating that even in areas with good protection, an increasing emission can still cause significant damage to the vegetation [22]. The vegetation vulnerability downstream increased from the base period to the near-term period and long-term period. There is Mara Mine downstream in MRB, and mining activities often grab the vegetation water [26], leading to insufficient vegetation water demand, and increasing vegetation vulnerability.

The terrain of the MRB is a gradual decrease from upstream to downstream, high altitude is not conducive to water aggregation [33], so the vegetation vulnerability decreased from upstream to downstream in all periods. The high temperature and little precipitation in tropical regions are highly

Preprints.org (www.preprints.org) | NOT PEER-REVIEWED | Posted: 4 March 2024 doi:10.20944/preprints202403.0044.v1

likely to increase the impact of drought on vegetation. Drought has an important impact on the vulnerability in the Masai Mara [34]. Also, an arid environment can reduce the growth rate of vegetation, this phenomenon can become more obvious when the emission increases [35]. Under the SSP5-8.5, regions that are already arid may become universally drought-stricken by the late 21st century [36], and the vegetation vulnerability will become much more intense.

5.2. Transition of Vegetation Vulnerability under Different Scenarios in the MRB

The stochastic matrix was used to quantitatively analyze the transition of vegetation vulnerability of different periods in the MRB. To our knowledge, it is the first time that the stochastic matrix has been used in vegetation vulnerability research. A Stochastic matrix was chosen because it can reflect the transition simply and directly [37].

Under the SSP1-2.6, the impact of human factors on vegetation vulnerability in MRB decreased and was less than the impact of natural factors. The climate will become warmer and wetter, making it more suitable for vegetation growth under the SSP1-2.6 [38], and the vegetation vulnerability will be the lowest [39]. Therefore, the vegetation vulnerability in the MRB increased a little from the base period to the near-term period, but slightly decreased from the near-term period to the long-term period.

Under the SSP2-4.5, the impact of natural and human factors on vegetation vulnerability in the near-term period was similar to the factors impact in the base period, but the impact of human factors on vegetation vulnerability in the long-term period increased by 14% compared to the base period in the MRB. Under the SSP2-4.5 scenario, moderate warming would lead to a slight drought [40], underdeveloped countries will face pressure from low education, high population growth, and intensified land use, including reduced forest and grassland [14]. For the MRB which is a low-developed area, the conflict environment of reduced vegetation, increased population, and regional competitions will make the increasing vegetation vulnerability.

Under the SSP5-8.5, the impact of human factors on vulnerability was 1.4 times greater than natural factors in the long-term period. The vegetation vulnerability in the long-term period increased by 950.00% compared to the base period, which was the highest vulnerability increase under all scenario assumptions. Under the SSP5-8.5 scenario, the population at risk of drought is projected to increase by 45.40 % in the 2050s, this will increase vulnerability in 80% of global land areas [41], resulting in severe vegetation damage. For the MRB which relies on agriculture and tourism to develop, increased vegetation vulnerability and damaged vegetation severely can seriously hinder further economic development.

The transition of vegetation vulnerability varied greatly under different scenarios. Under the sustainable SSP1-2.6, the increase in vegetation vulnerability was the smallest from the base period to the near-term period, and to the long-term period, the long-term vulnerability was 1.83 times that of the base period. Under the SSP5-8.5, vegetation vulnerability increased the most from the base period to the near-term period and to the long-term period, the long-term vulnerability was 9.5 times that of the base period. Therefore, sustainable development is of great significance for vegetation protection [42]. In the MRB where vegetation has been damaged due to socio-economic development, taking a low-emission development is an effective method to protect the vegetation environment.

6. Conclusion

This study assessed the vegetation vulnerability in the base period (2010-2019), near-term period (2020-2059), and long-term period (2060-2099) in the MRB, and then analyzed the transition of the vegetation vulnerability of different periods by stochastic matrix to point out the high vegetation vulnerability areas. The conclusions are as follows.

(1) The vegetation vulnerability in MRB in the base period showed a decreasing trend from east to west. The high-high cluster was with high vulnerability, the low-low cluster was with low vulnerability.

Preprints.org (www.preprints.org) | NOT PEER-REVIEWED | Posted: 4 March 2024 doi:10.20944/preprints202403.0044.v1

(2) In the near-term period and long-term period, vegetation vulnerability was highest upstream, followed by the downstream, and the lowest midstream. The vegetation vulnerability showed a high-high cluster in the east, while a low-low cluster in the midstream and downstream.

(3) The upstream of the MRB will experience the highest vegetation vulnerability increase due to intense human activity and less protection. The vegetation vulnerability decreased only under the SSP1-2.6, therefore, the MRB should control population growth, actively respond to climate change, and take the sustainable development path with low-emission to promote the sustainable vegetation in the MRB.

6. Patents

This section is not mandatory but may be added if there are patents resulting from the work reported in this manuscript.

Author Contributions: Wanyi Zhu and Zhenke Zhang designed the paper. Wanyi Zhu conducted the data processing and statistical analysis and wrote the paper. Shouming Feng and Hang Ren made great efforts in writing and figure optimization. All the authors contributed to the paper revision. All authors have read and agreed to the published version of the manuscript.

Funding: Authors acknowledge the support from the National key R&D projects (No. 2018YFE0105900).

Data Availability Statement: The ERA5-Land monthly averaged data from 2010 to 2019 are from the European Centre for Medium-Range Weather Forecasts (https://www.ecmwf.int/en/forecasts/datasets/reanalysis-datasets/era5, accessed on 10 February 2023). The CMIP6 data are also from the European Centre for Medium-Range Weather Forecasts (https://cds.climate.copernicus.eu/cdsapp#!/dataset/projections-cmip6?tab=form, accessed on 13 February 2023). The STRM data are from the Shuttle Radar Topography Mission (http://srtm.csi.cgiar.org, accessed on 20 February 2023). The land use data are from Land Use Harmonization 2(https://luh.umd.edu/data.shtml, accessed on 03 March 2023). The population data are from WorldPop(https://hub.worldpop.org/project/categories?id=18, accessed on 06 March 2023) and Our World in Data (https://ourworldindata.org/population-growth, accessed on 06 March 2023). The vegetation ecological water demand data are from the article (Zhu, W., Zhang, Z., Guo, X., Feng, S., JIANG, D., & JIANG, F. (2023) Characteristics and estimation of vegetation ecological water demand in the Mara River Basin. Acta Ecol. Sin, 43(18): 7523-7535.).

Acknowledgments: The authors are thankful for the generous support of the funding from National key R&D projects (No. 2018YFE0105900) and would like to thank the European Centre for Medium-Range Weather Forecasts, and NASA for their valuable data.

Conflicts of Interest: The authors declare no conflicts of interest.

References

1. Schwalm, C. R., Anderegg, W. R., Michalak, A. M., Fisher, J. B., Biondi, F., Koch, G., & Tian, H. Global patterns of drought recovery. Nature, 2017, 548(7666), 202-205.
2. Zhang, X., Yu, W., Cai, H., & Guo, X. Review of the evaluation methods of regional eco-environmental vulnerability. Acta Ecol. Sin, 2018, 38, 5970-5981.
3. Seaquist, J. W., Hickler, T., Eklundh, L., Ardö, J., & Heumann, B. W. Disentangling the effects of climate and people on Sahel vegetation dynamics. Biogeosciences, 2009, 6(3), 469-477.
4. Dai, X., Feng, H., Xiao, L., Zhou, J., Wang, Z., Zhang, J., ... & Yao, Y. Ecological vulnerability assessment of a China's representative mining city based on hyperspectral remote sensing. Ecological Indicators, 2022, 145, 109663.
5. Gonzalez, P., Neilson, R. P., Lenihan, J. M., & Drapek, R. J. Global patterns in the vulnerability of ecosystems to vegetation shifts due to climate change. Global Ecology and Biogeography, 2010, 19(6), 755-768.
6. Zhao, D., & Wu, S. Vulnerability of natural ecosystem in China under regional climate scenarios: an analysis based on eco-geographical regions. Journal of Geographical Sciences, 2014, 24, 237-248.
7. Turner, B.L., Kasperson, R.E., Matson, P.A., McCarthy, J.J., Corell, R.W., Christensen, L., Eckley, N., Kasperson, J.X., Luers, A., Martello, M.L. A framework for vulnerability analysis in sustainability science. Proc. Natl. Acad. Sci. 2003, 100, 8074–8079.

Preprints.org (www.preprints.org) | NOT PEER-REVIEWED | Posted: 4 March 2024 doi:10.20944/preprints202403.0044.v1

8. Wu, C., Liu, G., Huang, C., Liu, Q., & Guan, X. Ecological vulnerability assessment based on fuzzy analytical method and analytic hierarchy process in Yellow River Delta. International journal of environmental research and public health, 2018, 15(5), 855.
9. Ru, S. F., & Ma, R. H. Evaluation, spatial analysis and prediction of ecological environment vulnerability of Yellow River Basin. J. Nat. Resour, 2022, 37, 1722-1734.
10. Hyandye, C., Tao, W., & Hua, C. Z. Evaluation of eco-environmental vulnerability using RS and GIS: Case of Ma Keng iron mining area in Fu Jian Province, China. Environ. Res. J, 2008, 2(4), 196-204.
11. Bele, M. Y., Tiani, A. M., Somorin, O. A., & Sonwa, D. J. Exploring vulnerability and adaptation to climate change of communities in the forest zone of Cameroon. Climatic Change, 2013, 119(3-4), 875-889.
12. Nunes, J. P., Seixas, J., & Pacheco, N. R. Vulnerability of water resources, vegetation productivity and soil erosion to climate change in Mediterranean watersheds. Hydrological Processes: An International Journal, 2008, 22(16), 3115-3134.
13. Sitch, S., Huntingford, C., Gedney, N., Levy, P. E., Lomas, M., Piao, S. L., ... & Woodward, F. I. Evaluation of the terrestrial carbon cycle, future plant geography and climate-carbon cycle feedbacks using five Dynamic Global Vegetation Models (DGVMs). Global change biology, 2008, 14(9), 2015-2039.
14. O'Neill, B. C., Tebaldi, C., Van Vuuren, D. P., Eyring, V., Friedlingstein, P., Hurtt, G., ... & Sanderson, B. M. The scenario model intercomparison project (ScenarioMIP) for CMIP6. Geoscientific Model Development, 2016, 9(9), 3461-3482.
15. Popp, A., Calvin, K., Fujimori, S., Havlik, P., Humpenöder, F., Stehfest, E., ... & van Vuuren, D. P. (2017). Land-use futures in the shared socio-economic pathways. Global Environmental Change, 42, 331-345.
16. Fenta, A. A., Tsunekawa, A., Haregeweyn, N., Tsubo, M., Yasuda, H., Shimizu, K., ... & Sun, J. Cropland expansion outweighs the monetary effect of declining natural vegetation on ecosystem services in sub-Saharan Africa. Ecosystem Services, 2020, 45, 101154.
17. Mango, L. M., Melesse, A. M., McClain, M. E., Gann, D., & Setegn, S. Land use and climate change impacts on the hydrology of the upper Mara River Basin, Kenya: results of a modeling study to support better resource management. Hydrology and earth system sciences, 2011, 15(7), 2245-2258.
18. Mwemezi, B. R., & Luvara, V. G. Reliability of the environmental feasibility studies to the mining and construction projects: A case of Mara river basin in Tanzania. Am. J. Environ. Eng, 2017, 7, 65-72.
19. Zermoglio, F., Scott, O., & Said, M. Vulnerability and Adaptation Assessment in the Mara river basin. United States Agency for International Development, 2019, 102–105.
20. Inglada, J., & Mercier, G. A new statistical similarity measure for change detection in multitemporal SAR images and its extension to multiscale change analysis. IEEE transactions on geoscience and remote sensing, 2007, 45(5), 1432-1445.
21. Minale, A. S. Retrospective analysis of land cover and use dynamics in Gilgel Abbay Watershed by using GIS and remote sensing techniques, Northwestern Ethiopia. International Journal of Geosciences, 2013, 4(07), 1003.
22. del Río, S., Canas, R., Cano, E., Cano-Ortiz, A., Musarella, C., Pinto-Gomes, C., & Penas, A. Modelling the impacts of climate change on habitat suitability and vulnerability in deciduous forests in Spain. Ecological Indicators, 2021, 131, 108202.
23. Li, W., Buitenwerf, R., Munk, M., Bøcher, P. K., & Svenning, J. C. Deep-learning based high-resolution mapping shows woody vegetation densification in greater Maasai Mara ecosystem. Remote Sensing of Environment, 2010, 247, 111953.
24. Zhu, W., Zhang, Z., Zhao, S., Guo, X., Das, P., Feng, S., & Liu, B. Vegetation Greenness Trend in Dry Seasons and Its Responses to Temperature and Precipitation in Mara River Basin, Africa. ISPRS International Journal of Geo-Information, 2022, 11(8), 426.
25. Zhu, W., Zhang, Z., Guo, X., Feng, S., JIANG, D., & JIANG, F. Characteristics and estimation of vegetation ecological water demand in the Mara River Basin. Acta Ecol. Sin, 2023, 43(18): 7523-7535.
26. Mwangi, H. M., Julich, S., Patil, S. D., McDonald, M. A., & Feger, K. H. Modelling the impact of agroforestry on hydrology of Mara River Basin in East Africa. Hydrological Processes, 2016, 30(18), 3139-3155.
27. Bregoli, F., Crosato, A., Paron, P., & McClain, M. E. Humans reshape wetlands: Unveiling the last 100 years of morphological changes of the Mara Wetland, Tanzania. Science of the Total Environment, 2019, 691, 896-907.
28. Mati, B. M., Mutie, S., Gadain, H., Home, P., & Mtalo, F. Impacts of land-use/cover changes on the hydrology of the transboundary Mara River, Kenya/Tanzania. Lakes & Reservoirs: Research & Management, 2008, 13(2), 169-177.
29. Hu X, Ma C, Huang P, et al. Ecological vulnerability assessment based on AHP-PSR method and analysis of its single parameter sensitivity and spatial autocorrelation for ecological protection–A case of Weifang City, China. Ecological Indicators, 2021, 125: 107464.
30. He L, Shen J, Zhang Y. Ecological vulnerability assessment for ecological conservation and environmental management[J]. Journal of environmental management, 2018, 206: 1115-1125.

Preprints.org (www.preprints.org) | NOT PEER-REVIEWED | Posted: 4 March 2024 doi:10.20944/preprints202403.0044.v1

31. Blüthgen, N., Dormann, C. F., Prati, D., Klaus, V. H., Kleinebecker, T., Hölzel, N., ... & Weisser, W. W. A quantitative index of land-use intensity in grasslands: Integrating mowing, grazing and fertilization. Basic and Applied Ecology, 2012, 13(3), 207-220.
32. Dessu, S. B., Melesse, A. M., Bhat, M. G., & McClain, M. E. Assessment of water resources availability and demand in the Mara River Basin. Catena, 2014, 115, 104-114.
33. Ogutu, J. O., & Owen-Smith, N. ENSO, rainfall and temperature influences on extreme population declines among African savanna ungulates. Ecology Letters, 2003, 6(5): 412-419.
34. Galvin, K. A., Thornton, P. K., Boone, R. B., & Sunderland, J. Climate variability and impacts on East African livestock herders: the Maasai of Ngorongoro Conservation Area, Tanzania. African Journal of Range and Forage Science, 2004, 21(3), 183-189.
35. Bradford, J. B., Andrews, C. M., Robles, M. D., McCauley, L. A., Woolley, T. J., & Marshall, R. M. Landscape-scale restoration minimizes tree growth vulnerability to 21st century drought in a dry forest. Ecological Applications, 2021, 31(2), e2238.
36. Li, H., Li, Z., Chen, Y., **ang, Y., Liu, Y., Kayumba, P. M., & Li, X. Drylands face potential threat of robust drought in the CMIP6 SSPs scenarios. Environmental Research Letters, 2021, 16(11), 114004.
37. Perfect, H. Methods of constructing certain stochastic matrices.1953.
38. Chen, Z. T., Liu, H. Y., Xu, C. Y., Wu, X. C., Liang, B. Y., Cao, J., & Chen, D. Deep learning projects future warming-induced vegetation growth changes under SSP scenarios. Advances in Climate Change Research, 2022, 13(2), 251-257.
39. Ads, A., ale, S. M., & Khare, D. Vulnerability assessment of irrigation water requirement to climate change at Governorates level, Egypt. 2022.
40. Li, W., Buitenwerf, R., Munk, M., Amoke, I., Bøcher, P. K., & Svenning, J. C. Accelerating savanna degradation threatens the Maasai Mara socio-ecological system. Global environmental change, 2020, 60, 102030.
41. Wang, T., & Sun, F. Integrated drought vulnerability and risk assessment for future scenarios: An indicator based analysis. Science of The Total Environment, 2023, 900, 165591.
42. Ma, S., Qiao, Y. P., Wang, L. J., & Zhang, J. C. Terrain gradient variations in ecosystem services of different vegetation types in mountainous regions: Vegetation resource conservation and sustainable development. Forest Ecology and Management, 2021, 482, 118856.

Disclaimer/Publisher's Note: The statements, opinions and data contained in all publications are solely those of the individual author(s) and contributor(s) and not of MDPI and/or the editor(s). MDPI and/or the editor(s) disclaim responsibility for any injury to people or property resulting from any ideas, methods, instructions or products referred to in the content.